

Han Ul Lee · Dong-Woo Cho

An intelligent feedrate scheduling based on virtual machining

Received: 5 September 2002 / Accepted: 15 November 2002 / Published online: 23 July 2003
© Springer-Verlag London Limited 2003

Abstract Off-line feedrate scheduling is an advanced methodology to automatically determine optimum feedrates for NC code modification. However, most existing feedrate scheduling systems have limitations in generating the optimised feedrates because they use the material removal rate or the cutting force model which is dependent on cutting conditions. This paper proposes a feedrate scheduling system based on an improved cutting force model that can predict cutting forces accurately in general end milling situations. Original blocks of NC code were divided into smaller ones with the optimised feedrates to adjust the peak value of cutting forces to a constant value. The acceleration and deceleration characteristics for a given machine tool were considered for realistic feedrate scheduling. Moreover, a modified type of Z-map model was developed to reduce the entry/exit angle calculation error in the cutting force prediction and named the moving edge node Z-map (ME Z-map). Pocket machining experiments show that the proposed method is accurate and efficient in maintaining the cutting force at a desired level.

development period of a new product can be achieved. For this purpose, CAD/CAM systems were introduced and have been employed in machining industries. One of the major research issues in this area is directly related to reducing the machining time.

Feedrate scheduling has been one of the major topics in the CAM industry. When an operator uses an NC code generated by CAM software, it has to be modified because most existing CAM software generates the tool path only. The feedrate scheduling systems used in most CAM software have limitations in generating the optimised feedrates because they are based on the material removal rate (MRR) [1, 2]. This method works on a simple premise based on the cutting conditions and NC tool capacity; feedrates increase as less material is being removed and decrease as more material is being removed to keep the MRR constant. Optimum feedrates, however, cannot be obtained throughout the operation because the physical cutting force prediction is very difficult when only the MRR is used. That is, different cutting forces are generated under different cutting conditions even with the same MRRs. A feedrate scheduling model based on the cutting force prediction is thus required to obtain an effective and reliable feedrate.

Spence and Altintas [3] developed a 2 1/2 axis process simulation and planning system that utilises solid modellers for the workpiece geometry description. Feedrates are scheduled through the use of the tool/workpiece intersection data provided by the solid modeller and a flat end mill mechanistic model. To improve the cutting performance, Tarnag et al. [4] applied a geometric modelling system to an in-process simulation of the cutting geometry in pocket machining. The area of the chip cut was identified and then the corresponding cutting performance was evaluated and optimised. Lim and Menq [5] created an integrated planner for machining complex surfaces that optimised the cutting path and the feedrate. Research work on feedrate optimisation by Chu et al. [6] indicated that static and dynamic cutting characteristics change dramatically for different local shape features. The

1 Introduction

A cutting process using a machine tool is very common in many industries, e.g., the aerospace, automobile and die-mould industries. The cutting process accounts for a large part of the development and manufacturing of most products. Thus, by reducing the time needed for this cutting process, higher productivity and a shorter

H. U. Lee · D.-W. Cho (✉)
Department of Mechanical Engineering,
Pohang University of Science and Technology,
San 31 Hyoja-dong, Nam-gu, 790-784 Pohang,
Kyungbuk, S. Korea
E-mail: dwcho@postech.ac.kr

relationship between the optimal feedrate and the local shape feature was established through various experiments. Feng and Su [7] presented an integrated approach for the concurrent optimisation of the tool path and feedrate for the finishing machining of 3D plane surfaces using ball-end milling. Fussell et al. [8] developed a feedrate process planner for complex sculptured end milling cuts from mechanistic and geometric end milling models. The selection program used tool deflection, surface finish, tool failure and machine power data to set constraints on the cutting force and the feed-per-tooth for rough, semi-finish and finish passes. However, the present cutting force models have limitations in generating the scheduled feedrates because they are based on the cutting force model which is dependent on cutting conditions.

In contrast, this paper presents a feedrate scheduling system based on an improved cutting force model [9, 10] that can predict cutting forces precisely in general machining situations. The next section describes the mechanistic and geometric simulations of end milling. To reduce calculation errors in geometric simulation, a modified type of Z-map model was developed and named ME Z-map. The feedrate scheduling method composed of the feedrate optimisation and NC code modification models is then described in a later section. The acceleration and deceleration characteristics for a given machine tool were considered for realistic feedrate scheduling. Experimental results of the proposed feedrate scheduling are then presented and discussed, along with conclusions.

2 The cutting process simulation

In order to simulate the cutting process of end milling for a given set of NC code, a geometric model and a cutting force model are needed. The geometric model calculates the shape of the workpiece and the cutting configurations. Cutting configuration is a term used to represent the nominal position and entry/exit angle of a cutter, cutting conditions, and feed direction at the nominal cutter position, during machining. Using these data, the cutting force model predicts the cutting forces. In this paper, the cutting forces in end milling are predicted using the model developed by Yun and Cho [9, 10]. For a more efficient cutting process simulation, a new Z-map model, called the ME Z-map model, was developed to simultaneously compute the cutting configurations more accurately and to reduce the computing time.

2.1 An improved cutting force model

The end milling cutter is divided into a finite number of disk elements and the total x -, y -, and z -force components acting on a flute at a particular instant are obtained by summing up the force components acting on each individual disk element. Subsequently, a summa-

tion of all flutes engaged in the cut yields the total forces acting on the cutter at that particular time instant. Figure 1 shows the cross section of the cutter geometry and defines the coordinate system to be used for analysis. The angular position ($\phi(i,j,k)$) of the k -th axial disk element of the i -th flute at the j -th angular position ($\theta(j)$) of the cutter is given by Eqs. 1, 2, and 3:

$$\phi(i,j,k) = \alpha(i,k) + \theta(j) \quad (1)$$

$$\alpha(i,k) = (i-1)\phi_c + (k\Delta a + \Delta a/2) \frac{\tan \theta_h}{r} \quad (2)$$

$$\theta(j) = -j\Delta\theta, \quad (3)$$

where $\alpha(i,k)$ is the cutting edge location angle at $j=0$, ϕ_c is the flute spacing angle and θ_h is the helix angle.

In flat end milling, the cutting force components at the j -th angular position can be described as follows:

$$\begin{aligned} F_x(j) &= \sum_k \sum_i [C_1 \cos(\phi - \alpha_r) + K_f C_3 \cos \phi \\ &\quad - K_f C_4 \sin(\phi - \alpha_r)] K_n B_1 t_c(\phi) \\ F_y(j) &= \sum_k \sum_i [C_1 \sin(\phi - \alpha_r) + K_f C_3 \sin \phi \\ &\quad - K_f C_4 \cos(\phi - \alpha_r)] K_n B_1 t_c(\phi) \\ F_z(j) &= \sum_k \sum_i [-C_2 + K_f C_5] K_n B_1 t_c(\phi) \end{aligned} \quad (4)$$

$$C_1 = \cos \theta_h / \sin \theta_{tk}$$

$$C_2 = (\sin \theta_h / \sin \theta_{tk}) \cos \alpha_r$$

$$C_3 = \sin \theta_h (\sin \theta_c - \cos \theta_c \cot \theta_{tk})$$

$$C_4 = \cos \theta_c / \sin \theta_{tk}$$

$$C_5 = \cos \theta_h (\sin \theta_c - \cos \theta_c \cot \theta_{tk})$$

$$\cos \theta_{tk} = \sin \alpha_r \cdot \sin \theta_h$$

where α_r is the rake angle, t_c is the uncut chip thickness and K_n , K_f , and θ_c are the cutting force coefficients—the

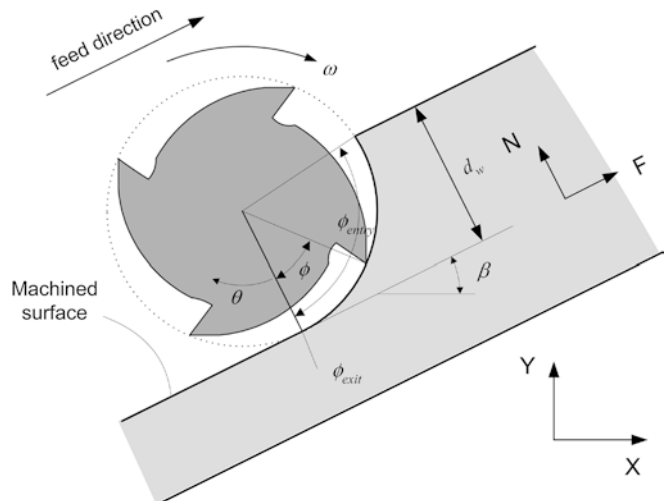


Fig. 1 The two-dimensional milling process geometry of a disk element [10]. Note that N and F are the normal direction of the machined surface and the feed direction, respectively

normal specific cutting force, the frictional specific cutting force, and the chip flow angle, respectively.

In Eq. 4, C_1 , C_2 are constant values while C_3, C_4 , and C_5 are functions of the chip flow angle (θ_c).

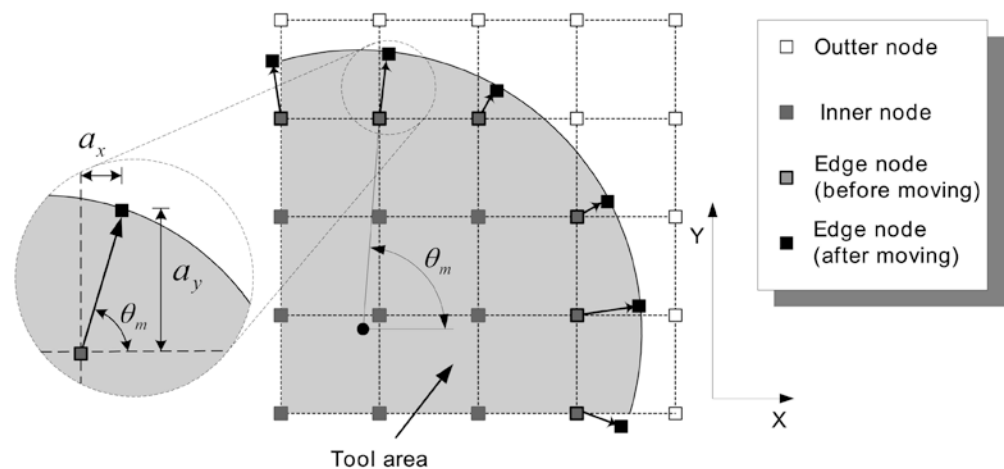
The instantaneous uncut chip thickness can be calculated as a function of the position of the centre of the cutter for each z -axis disk element. The position of the centre of the cutter deviates from its nominal position due to numerous factors such as the cutter deflection, the runout, the servo error, the volumetric error, the thermal error and wear. Of all these factors, cutter deflection and runout account for the largest contribution to the cutter deviation. Thus, the actual position of the centre of the cutter, (x_a, y_a) , can be realistically represented by:

$$\begin{aligned} x_a(j, k) &= x_n(j) + x_\rho(j) + x_d(j, k) \\ y_a(j, k) &= y_n(j) + y_\rho(j) + y_d(j, k) \end{aligned} \quad (5)$$

where (x_n, y_n) is the nominal position of a cutter and (x_ρ, y_ρ) and (x_d, y_d) are the deviations caused by the cutter runout and the deflection, respectively. The instantaneous uncut chip thickness, defined as the distance between the path that the current tooth of interest is generating and the exposed workpiece surface generated by the previous tooth, can therefore be estimated from the position of the centre of the cutter [9].

The cutting force model needs to consider the size effect for a better prediction accuracy of the cutting forces. The size effect refers to the increase in the specific cutting force for the small values of the uncut chip thickness. To strictly consider the size effect, a nonlinear relationship between the cutting coefficients and the uncut chip thickness ($t_c(i, j, k)$) at every k -th axial disk element of the i -th flute at the j -th angular position of the cutter is required. Using the fitted result for the uncut chip thickness and the cutting coefficients, this relationship can be readily derived in the form of the Weibull function. Instead of a normal uncut chip thickness, a re-scaled one [10] is used for an accurate and effective fitting. A good prediction is able to be obtained when the cutting coefficients, in which the size effect model is included, are used.

Fig. 2 A fundamental notion for the ME Z-map



2.2 An ME Z-map model

For analysis, the resolution of the existing Z-map models depends on the number of nodes, and these models cannot describe the cutter boundary between grids. To enhance the resolution of the Z-map, the number of nodes must be increased, which in turn increases the computational burden. When the radial depth of cut is less than the grid size and there is no node in machining region, a substantial error is especially induced in the cutting configuration or the cutting force calculation. This paper presents the ME Z-map model that produces a more accurate cutting configuration and which can be applied to a small depth of cut.

2.2.1 The fundamental notions of the ME Z-map model

One inherent weakness of the conventional Z-map model is that the geometric variation between two nodes is entirely unknown due to the fixed grid size and its position.

As illustrated in Fig. 2, a fundamental notion for the ME Z-map is to move the edge node (the node closest to the cutter edge) towards the boundary of the cutter movement. The edge node moves in the direction of θ_m which is the angle of the edge node from the cutter centre, so that the coordinate of node (i, j) is changed to:

$$\begin{aligned} x &= i \cdot g + a_x \\ y &= j \cdot g + a_y \end{aligned} \quad (6)$$

where g is the elemental grid size, and a_x and a_y are the distances moved from the original coordinates. The values of a_x and a_y should be smaller than the elemental grid size.

In the simulation process, every node position is calculated one after another and the node located in the edge area is defined as the edge node, as illustrated in Fig. 3a. Figure 3b shows that the boundary of the swept volume can be described precisely by moving the edge nodes during machining. In the ME Z-map model, the

edge nodes are designated only in the boundary region of the swept volume; conventional nodes are used in other regions.

2.2.2 A comparison between the Z-map and the ME Z-map

In order to evaluate the performance of the ME Z-map, an arbitrary transient cut as illustrated in Fig. 4 is simulated. Figure 4 shows the examples of a transient cut in the 2D end milling process which is formed by the line path, the arc path, the intersection of a line and arc path and the transient cut where the cutting depth continuously changes. Entry and exit angles computed using the ME Z-map and the conventional Z-map are presented in Fig. 5. For a large grid size, the conventional Z-map produces a significant error in the entry and exit angle calculation, whereas the ME Z-map produces quite accurate values, regardless of the grid size.

Throughout this comparison, it was found that the ME Z-map produces more accurate cutting configurations than the conventional Z-map, even with a five to ten times larger grid size, which requires a dramatically shorter computing time.

3 The feedrate scheduling

The feedrate scheduling described in this paper consists of two steps: the first step is the calculation of an optimised feedrate based on a reference cutting force and the second step is the modification of NC code to accommodate these feedrates.

3.1 The feedrate optimisation

3.1.1 Overview

Generally, machining using end milling is classified into three steps: rough milling, semi-finish milling, and finish

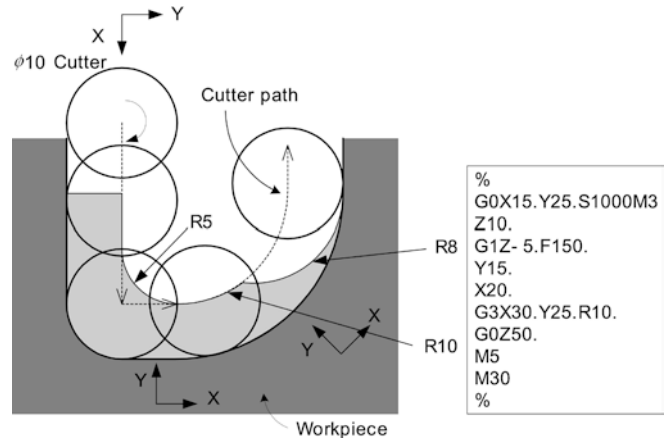


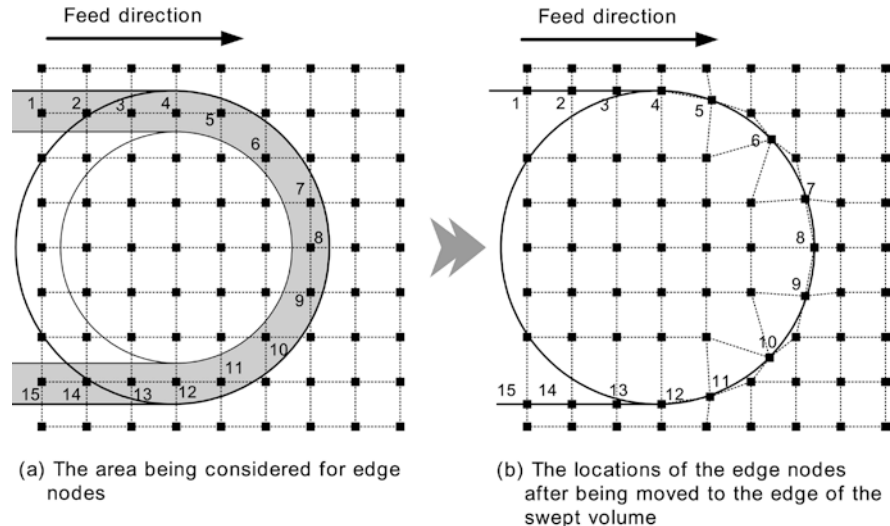
Fig. 4 An example of a transient cut in the 2D end milling process for a comparison between the Z-map and the ME Z-map

milling. In rough and semi-finish milling, machining time is the most important factor for better productivity. Thus, the feedrate scheduling in this case aims at reducing the machining time. In finish milling, on the other hand, dimensional tolerance is the dominant factor for productivity. The aim of feedrate scheduling for finish milling is thus to minimise the machined surface errors.

As mentioned before, in rough and semi-finish milling, the feedrate must be maximised to minimise the machining time. However, the faster the feedrate is, the larger the cutting force becomes. Increased cutting force produces various problems such as machining chatter, tool wear and breakage. Thus, the strength of the cutting tool is usually the main constraint. In flat end milling, it is the resultant force of F_n and F_f that affects the above-mentioned problems, whereas it is the resultant force of F_n , F_f and F_z in ball end milling. Here, F_n and F_f are the cutting forces normal for the machined surface and the feed directional cutting force, respectively, as shown in Fig. 1.

In finish milling, machined surface error is a more important factor than machining time for feedrate

Fig. 3 The generation of the edge nodes in the ME Z-map



(a) The area being considered for edge nodes (b) The locations of the edge nodes after being moved to the edge of the swept volume

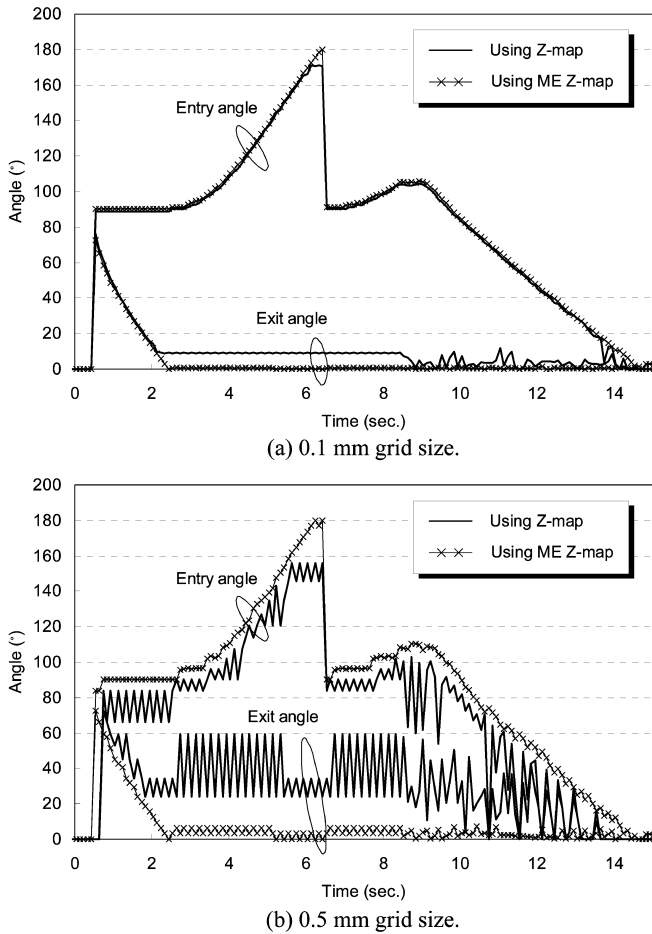


Fig. 5 A comparison of the entry and exit angles calculated using the Z-map and the ME Z-map in the case of Fig. 4

scheduling. The cutter deflection caused by the cutting force in end milling is the main cause for machined surface error. Thus, the tool deflection should not be larger than a preset tolerance in the feedrate scheduling for minimising the surface error. This paper presents a feedrate scheduling method for flat end milling that minimises the machining time. The resultant force of F_n and F_f is adopted as a criterion for feedrate scheduling.

3.1.2 A feedrate optimisation model

The relationship between the cutting force and the feedrate cannot be formulated in a closed form when the cutting force model includes the tool deflection, the run-out and the size effect, because the uncut chip thickness and cutting coefficients are altered by the previous cutting force even if the cutting conditions are fixed. In this paper, an iterative approach presented in the flowchart of Fig. 6 is used for the feedrate optimisation using the improved cutting force model.

The feedrate optimisation begins with an initial trial feedrate. The cutting force is calculated for this feedrate, and compared with the reference cutting force. If the difference is significant, a new trial feedrate is

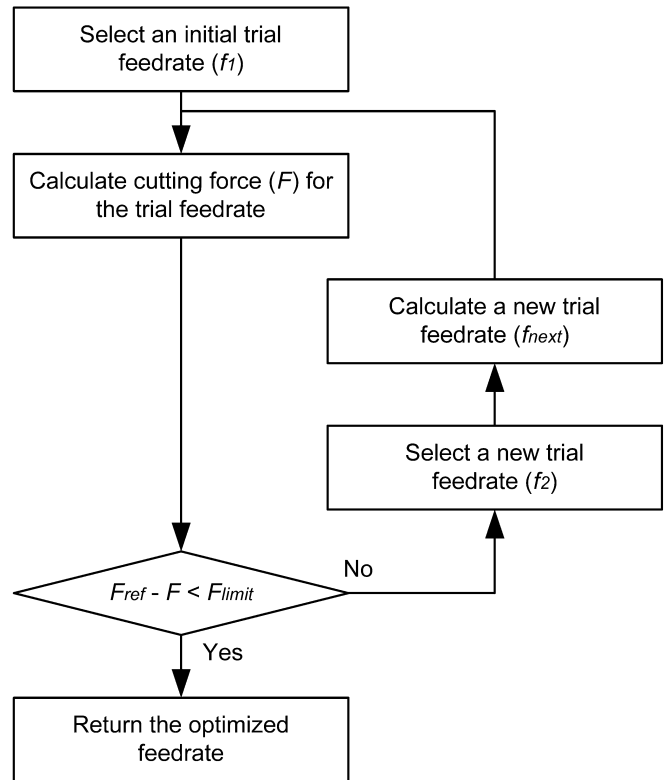


Fig. 6 An algorithm for the feedrate optimisation

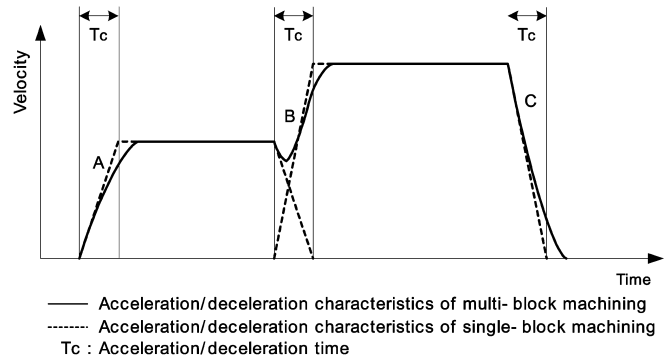


Fig. 7 The acceleration and deceleration characteristics of a machine tool

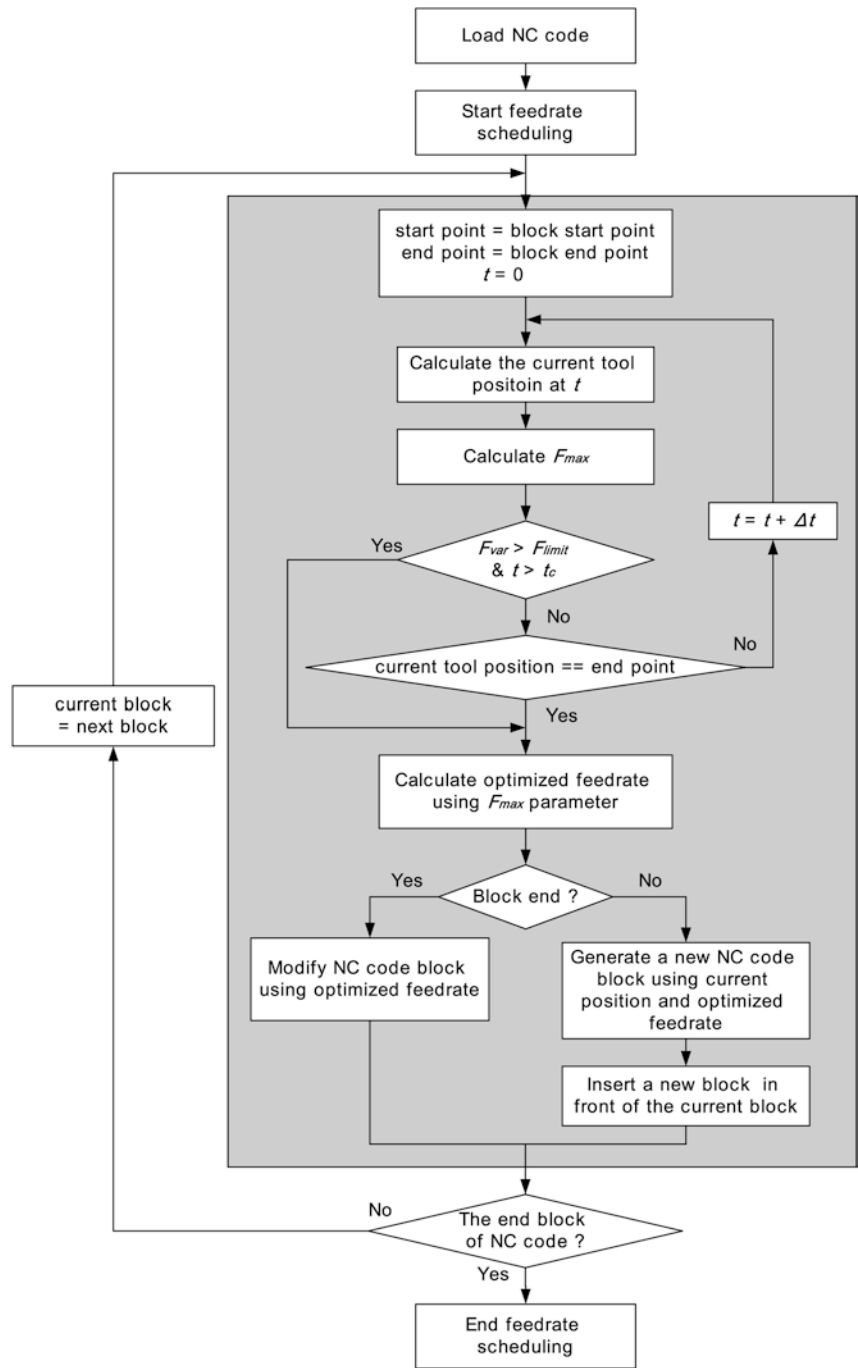
used to calculate the cutting force, which is then compared with the reference cutting force again. The new trial feedrate can be calculated using Eq. 7 under the assumption that the feedrate has a linear relationship with the cutting force:

$$f_{next} = f_1 + \frac{(F_{ref} - F_1)(f_2 - f_1)}{F_2 - F_1} \quad (7)$$

where F_1 and F_2 are the maximum resultant cutting forces when the feedrates are f_1 and f_2 , respectively, and F_{ref} is the reference resultant cutting force.

This process is repeated until the difference falls within a preset tolerance. The optimised feedrate is

Fig. 8 An algorithm for NC code modification



iteratively determined in this manner as illustrated in Fig. 6.

3.2 The NC code modification

3.2.1 An outline of the proposed modification scheme

In order to apply the optimised feedrates to actual machining, the original NC code must be properly modified. The modification consists of two steps: firstly, each block of NC code is divided according to cutting

force variation, and secondly, an optimised feedrate is inserted in the divided block of NC code.

The algorithm for the NC code modification begins by determining the reference value of the resultant cutting force and the limit on the cutting force variation. If the cutting force variation exceeds the limit, then the modification system automatically divides the NC code and inserts a new feedrate which sets the resultant cutting force at a reference value. In machining using the modified NC code based on this algorithm, the cutting force can be maintained at a constant value.

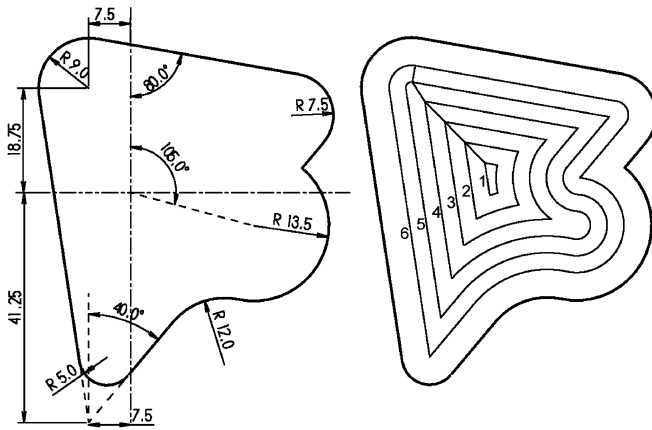


Fig. 9 The workpiece geometry and the tool path for pocket machining. Loop numbers are given in the diagram on the right

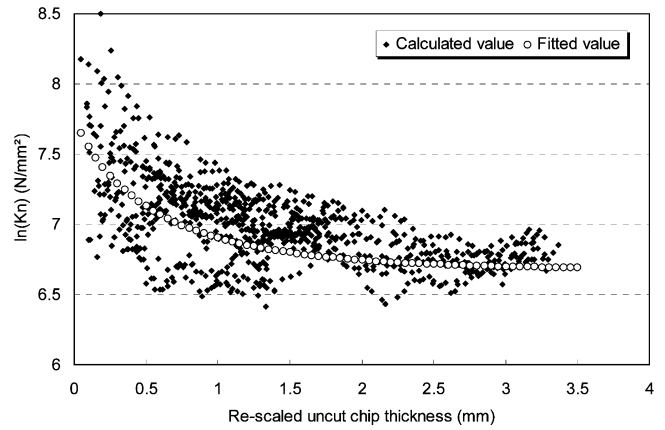
Table 1 The curve-fitting results using Eq. 8 for the re-scaled uncut chip thickness and the cutting coefficients

	A	B	d	k
$\ln(K_n)$	6.80602	7.79393	0.81730	1.76661
K_f	7.75202	2.17832	1.13515	1.82361
θ_c	0.50683	0.28578	4.66246	0.90926

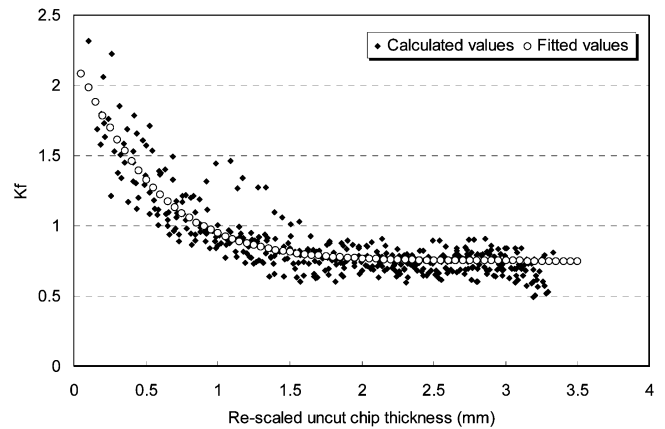
3.2.2 A consideration of the acceleration and deceleration characteristics of the machine tool

Acceleration and deceleration profiles managed by a CNC controller have the form of exponential functions such as the solid line graphs in the A and C regions in Fig. 7 [11]. Due to these profiles, it takes somewhat longer than the preset acceleration/deceleration time of the given machine tool to reach the commanded feedrate. For a smooth change of velocity, the feedrate is attained by overlapping the acceleration and deceleration parts of the respective blocks, as shown in Fig. 7. Consequently, all blocks in the NC code should always allow a fixed acceleration/deceleration time to achieve target values. In later models of the machine tools, this problem is resolved by a Look Ahead control. However, the acceleration/deceleration characteristics still have to be considered because a feedrate profile of a step function form is not achievable in any machine tool.

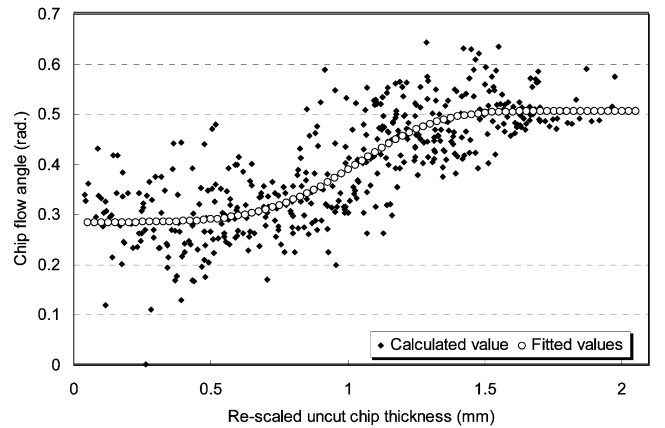
If the machining time of a certain block is shorter than the acceleration/deceleration time, the feedrate never reaches the commanded value. In fact, each divided block size has to be at least 2 or 3 times larger than the acceleration/deceleration time in order to allow the feedrate to become steady. As the block size becomes larger, a longer steady feedrate portion can be obtained. In this paper, NC code blocks are divided when the following two conditions are simultaneously satisfied. The first condition is that the cutting force variation exceeds the limit value, and the second condition is that the size of the new block to be inserted should be larger than the acceleration/deceleration time.



(a) $\ln(K_n)$



(b) K_f



(c) θ_c

Fig. 10 A comparison of cutting coefficients before and after the fitting by the Weibull function (Eq. 8) with respect to the re-scaled uncut chip thickness. Note that the calculated values are obtained from actual measurements

3.2.3 An algorithm for the NC code modification

As schematically illustrated in Fig. 8, NC code modification begins with the loading of NC code, after which each block in the NC code is simulated one by one. While the cutting forces in the block currently being simulated are calculated, a new block whose end point is the current tool position is inserted in front of

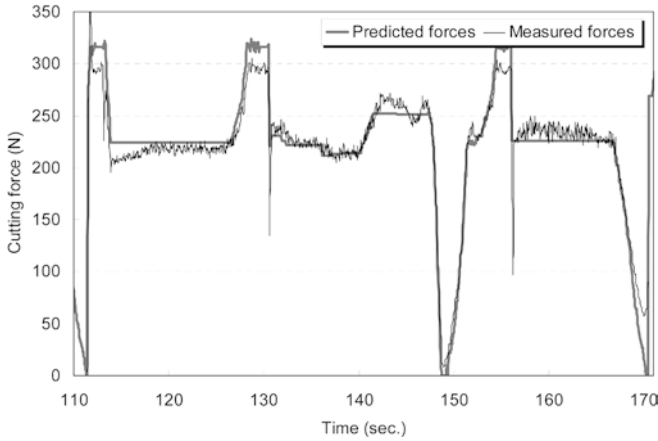


Fig. 11 A comparison between the measured and predicted maximum resultant cutting forces for loop 5

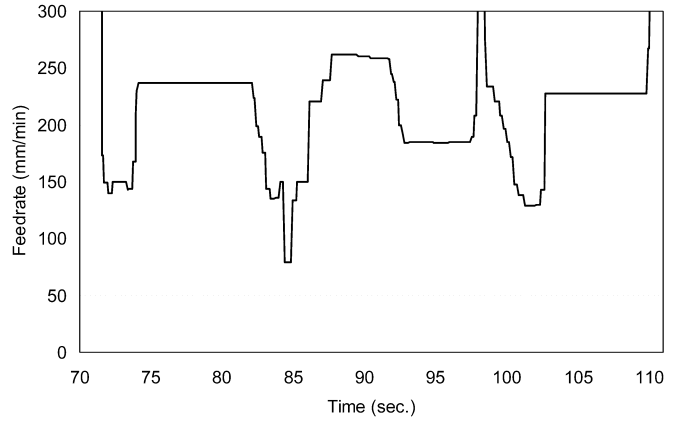


Fig. 12 The optimised feedrate for loop 5

Table 2 A comparison of the NC code before and after the feedrate scheduling for loop 5

Before the feedrate scheduling	After the feedrate scheduling
N174X17.674Y62.735 N176G3X17.5Y62.75R1.	N174X17.674Y62.735F150 N176G3X17.5Y62.75R1.F143 G3X16.818Y62.482J-1.000F144 G3X16.502Y61.821I0.682J-0.731F168
N178X16.5Y61.75R1. N180X16.511Y61.6R1.	N178X16.5Y61.75R1.F211 N180X16.511Y61.6R1.F230 G1X21.311Y29.962F237 G1X21.423Y29.220F224 G1X21.536Y28.478F199
...	...
N182G1X22.753Y20.457	G1X22.324Y23.285F79 G1X22.436Y22.543F134 N182G1X22.753Y20.457F150 G1X23.235Y21.031F221 G1X25.003Y23.137F221 G1X25.806Y24.095F239
N184X26.545Y24.975	N184X26.545Y24.975F239 G2X32.984Y30.039I15.321J-12.856F262 G2X35.524Y31.087I8.881J-17.920F260 G2X36.480Y31.380I6.342J-18.968F260 G2X39.916Y32.024I3.683J-19.658F259
N186G2X41.866Y32.119R20.	N186G2X41.866Y32.119R20.F259 G2X42.616Y32.105I-0.001J-20.000F258 G2X43.365Y32.063I-0.752J-19.986F245 G2X44.112Y31.993I-1.503J-19.943F238 G2X44.855Y31.895I-2.254J-19.873F222 G2X45.594Y31.768I-3.004J-19.773F200
N188X45.999Y31.687R20. N190G3X47.136Y31.569R5.5	N188X45.999Y31.687R20.F193 N190G3X47.136Y31.569R5.5F184 G3X51.624Y33.890I-0.000J5.500F185 N192X52.636Y37.069R5.5F184
N192X52.636Y37.069R5.5	G3X50.709Y41.250I-5-500J0.000F185 G3X50.107Y41.697I-3.574J-4.181F190 G3X49.450Y42.058I-2.972J-4.628F208 G3X48.750Y42.327I-2.316J-4.989F307 G3X48.020Y42.498I-1.614J-5.258F932
N194X47.517Y42.556R5.5	N194X47.517Y42.556R5.5F4000 G2X45.223Y43.892I2.014J2.223F4000 G2X44.891Y44.562I2.501J1.657F2100 G2X44.735Y45.294I2.833J0.987F1345
N196G2X44.724Y45.548R3.	N196G2X44.724Y45.548R3.F813
...	...

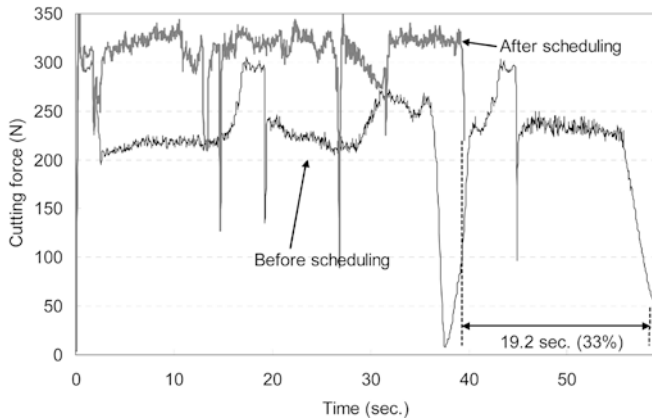


Fig. 13 A comparison of the maximum resultant cutting force before and after the feedrate scheduling for loop 5

the current block if both the cutting force variation and the block size are larger than the limit values. The optimised feedrate of the created block is calculated based on the maximum values of the cutting force. When the current tool position during simulation reaches the end point of the current block, the new optimal feedrate is calculated and replaces the present one. After modifying the current block, the feedrate scheduling system loops back to schedule the next block.

4 The feedrate scheduling results

In order to evaluate the proposed feedrate scheduling method, it was applied to an arbitrary pocket machining operation. The measured and predicted maximum resultant cutting forces were compared to show the accuracy of the proposed cutting process simulation method.

4.1 Experiments

The shape of an example pocket machining is composed of various paths such as the intersection of line-line, line-arc, and arc-arc shown in Fig. 9. The tool path was generated by commercial CAM software (CNC Software, Inc., Mastercam). The offset value in the tool path and the initial feedrate were set at 3 mm and 150 mm/min, respectively, and the cutter diameter was 10 mm. The generated NC code consisted of 78 lines and the total machining time was 240.1 seconds.

In order to evaluate the proposed feedrate scheduling system, cutting forces were measured during machining. The experiment was conducted with an HSS flat end mill with four flutes on a vertical type-machining centre (Daewoo Heavy Industry Ltd., ACE-V30). A tool dynamometer (Kistler, type 9257A) was used to measure the cutting forces and the workpiece material was aluminium 2014-T6.

4.2 The feedrate scheduling results and an evaluation

In order to consider the size effect in the cutting force model, the relationship between uncut chip thicknesses (t_c) and cutting coefficients were expressed through the Weibull function, given by Eq. 8:

$$y = A - (A - B)e^{-kx^d} \quad (8)$$

The fitted results for t_c and cutting coefficients, $\ln(K_n)$, K_f , and θ_c , calculated using the processed cutting forces, are shown in Table 1. Figures 10a–c show the values of $\ln(K_n)$, K_f , and θ_c , individually calculated from the measured cutting forces with respect to t_c , together with the fitted values of $\ln(K_n)$, K_f , and θ_c , respectively.

For the fifth loop of tool paths for pocket machining in Fig. 9, the simulation results were compared with the experimental results in Fig. 11. It can be seen that predicted maximum resultant cutting forces are in good agreement with the measured values. The modified NC code is compared with the original NC code in Table 2, and optimised feedrates of the fifth loop are shown in Fig. 12. By using the proposed feedrate scheduling, the number of the entire NC lines of code was increased from 78 to 377 while the total machining time was reduced from 240.1 seconds to 155.5 seconds, a savings of about 35%. Figure 13 is a comparison of the maximum resultant cutting force before and after the feedrate scheduling for loop 5. It is clearly seen that the maximum resultant cutting force obtained from the proposed optimally scheduled feedrates is more uniform than that from the fixed feedrate.

5 Conclusions

In this paper, a new feedrate scheduling system was presented based on an improved cutting force model that can predict cutting forces accurately in general machining situations. The feedrate was optimised to maintain the cutting forces at a specified level by the proposed feedrate optimisation method and then was inserted into a current NC code block by an NC code modification method. Original blocks of NC code were divided into smaller ones with the optimised feedrate to adjust the cutting force to a constant value. The acceleration and deceleration characteristics of a given machine tool were considered when the feedrate scheduling was performed. A modified ME Z-map model was developed to reduce the entry/exit angle calculation error in the cutting force prediction. The proposed NC code modification method was applied to an arbitrary type of pocket machining operation. The machining time was shown to be reduced by 35% when compared to the time for non-scheduled machining. Experimental results also show the accuracy and the effectiveness of the proposed feedrate scheduling method in maintaining the cutting force at a desired level.

Acknowledgements This work was supported by the Korean Research Foundation, grant no. KRF-2000-041-E00092.

References

1. Wang WP (1988) Solid modeling for optimizing metal removal of three-dimensional NC end milling. *J Manufact Sys* 7(1):57–65
2. Jang DJ, Kim KS, Jung JM (2000) Voexl-based virtual multi-axis machining. *Int J Adv Manufact Technol* 16(10):709–713
3. Spence AD, Altintas Y (1994) A solid modeller based milling process simulation and planning system. *J Engin Indust* 116:61–69
4. Tarnq YS, Shyur YY, Lee BY (1995) Computer-aided generation of the cutting conditions in pocket machining. *J Mater Process Technol* 51:223–234
5. Lim EM, Menq CH (1997) Integrated planning for precision machining of complex surfaces. Part 1: cutting-path and feedrate optimization. *Int J Mach Tool Manufact* 37(1):61–75
6. Chu CN, Kim SY, Lee JM, Kim BH (1997) Feed-rate optimization of ball end milling considered local shape features. *Annals CIRP* 46(1):433–436
7. Feng HY, Su N (2000) Integrated tool path and feedrate optimization for the finishing machining of 3D plane surfaces. *Int J Mach Tool Manufact* 40:1557–1572
8. Fussell BK, Jerard RB, Hemmett JG (2001) Robust feedrate selection for 3-axis NC machining using discrete models. *J Manufact Sci Engin* 123:214–224
9. Yun WS, Cho DW (2000) An improved method for the determination of 3D cutting force coefficients and runout parameters in end milling. *Int J Adv Manufact Technol* 116(12):851–858
10. Yun WS, Cho DW (2000) An improved cutting force model considering the size effect in end milling. In: *Proceedings of the ASME International Mechanical Engineering Congress and Exposition, Orlando, Florida, 5–10 November 2000*
11. The outline of the machining center and NC programming manual. Daewoo Heavy Industry, Ltd.